Influence of the colloidal processing route on the mechanical properties of Ti(C,N)-based cermets

M. Dios*, Z. Gonzalez**, B. Ferrari**, I. Kraleva***, R. Bermejo****, P. Alvaredo*, E. Gordo*

* University Carlos III of Madrid, IAAB, Leganes, Madrid, Spain

** Institute of Ceramic and Glass, CSIC, Madrid, Spain

*** Materials Center Leoben Forschung GmbH, Leoben, Austria

**** Institut für Struktur- und Funktionskeramik, Montanuniversität Leoben, Leoben, Austria

"Presented at the 19th Plansee Seminar, 29 May – 2 June, 2017"

Abstract

Cermets constituted by 85 vol.% Ti(C,N) and a Fe-Ni alloy as metal matrix present a great potential due to its combination of properties, such as high wear and oxidation resistance, together with high values of hardness. In this work, colloidal techniques are proposed as alternative processing method that permits to obtain highly dispersed phases in an aqueous media, avoiding milling, and leading to homogeneous microstructures. These techniques also permit a variety of forming methods. Stable aqueous suspensions of Fe-Ni powders and Ti(C,N) particles have been prepared and different forming methods were used to obtain bulk samples: Slip casting (SC); Slip Casting + Cold Isostatic Pressing (SC-CIP); Spray-Dry + Uniaxial Pressing (SDP). The SD provides spherical granules with high compressibility able to be shaped by uniaxial pressing. All the samples prepared were sintered in vacuum to near full density. The mechanical strength was determined by biaxial bending performed on discs using the ball-on-three-balls (B3B) method, with the subsequent fractographic analysis to investigate the effect of the processing route. The fracture resistance was measured on Single Edge V-Notched Beam (SEVNB) specimens fabricated through SDP tested under 4-point-bending.

Keywords

Colloidal Processing, Powder Metallurgy, Ti(C,N)-based cermet, FeNi, Biaxial strength, Fracture resistance

Introduction

Up to date, numerous practical machining operations and several progresses have been made in various cutting tool materials. Among them, Ti(C,N)-based cermets have received significant attention, being considered as one of the most promising candidates [1, 2]. Compared to traditional cemented carbides

(WC-Co), cermet materials have been widely used to prepare advanced ceramic composites applied in electrical, electronic, automotive and refractory industries thanks to their excellent and unique combination of physical properties such as high melting point, hardness at high temperature, strength, wear and oxidation resistance and thermal conductivity [3].

In the production of cermets, the starting materials are typically Ti(C,N) together with a metal binder which usually includes Ni, Co or a combination of both [3]. Other studies have proposed the use of iron as a promising matrix for these composite materials serving as an alternative to replace the toxic and expensive traditional binder composition. The advantages in the use of iron as metal matrix are related with its lower toxicity and price [4] as well as the ability to be hardened by heat treatment [5]. The main shortcoming observed in the processing of Fe-matrix cermets is the poor wettability on Ti(C,N) particles during sintering in the liquid phase, which can be improved by the addition of alloying elements and compounds such as Mo2C, Cr, Mo or Ni [6–8]. Specially the addition of a small amount of Ni improves noticeably the wetting behavior between both phases, as has been reported elsewhere [9].

The most common route used for the preparation of the starting cermet powders is the conventional powder metallurgy route, which imply the milling of powders for long times (up to 7 days in a ball mill) using an organic media as ethanol or isopropanol and binder lubricants such as paraffin wax. Other alternatives have been explored such as, for example the self-propagating high temperature synthesis (SHS) [10, 11], or the mechanical induced self-sustaining reaction (MSR) [12]. The resulting powders have been successfully employed in the production of Ti(C,N) cermets by pressureless sintering [13, 14], spark plasma sintering [15], hot pressing [12], hot isostatic pressing (HIP), or a combination of sintering and HIP, under different atmospheres (Vacuum, N_2, Ar) [16]. However it is very challenging to get uniform and homogeneous microstructures, as well as avoid the grain growth and hard phase cluster formation when the cermets are processed through agglomeration and sintering or SHS, HIP and SPS processes.

In an attempt to obtain a well-controlled microstructure and a better dispersion of phases with lower energy consumption than the rest of the conventional techniques, colloidal processing emerges as an alternative for the preparation of cermet materials. Aqueous colloidal processing allows obtaining homogeneous composite materials with complex shapes and structures, minimizing processing defects [17–19]. The success of this processing approach is based on two main interrelated factors. The first one is the control of the interparticle potentials in order to achieve high repulsions between particles, preventing the agglomeration and obtaining good dispersions. The second factor is the rheology optimization of the suspensions, which depends on the level of repulsions of the particles in the media as well as on other variables such as solid content and processing additives [20, 21].

In this work, stable aqueous suspensions of Fe-Ni powders and Ti(C,N) particles have been prepared combining colloidal processing and powder metallurgy techniques. After an initial characterization of the starting commercial powders and the rheological characterization of the suspensions prepared from those powders, colloidal and powder metallurgy techniques were combined to obtain bulk samples through different forming methods: Slip Casting (SC); Slip Casting + Cold Isostatic Pressing (SC-CIP) and Spray-Dry + Uniaxial pressing of the spherical granules generated (SDP). In order to avoid the addition of secondary carbides, a small amount of Ni (15 wt.%) was added in this work. The effect of the processing route on the strength and fracture resistance was investigated. A microstructural and

fractographic analysis was performed on selected specimens, showing appreciable differences depending on the processing route. Biaxial strength was determined in all samples using the ball-on-three-balls (B3B) method on disc-shaped specimens. Single Edge V-Notched Beam (SEVNB) specimens were tested under four-point-bending (4PB) in order to obtain the fracture resistance.

Experimental

Characterization of the starting powders and preparation of samples

Powders used in this study were titanium carbonitride (Ti(C,N), $Ti(C_{0.5},N_{0.5})$ Grade C) and iron (Fe, Fe SM) both provided by H.C. Starck (Germany) and nickel (Ni, Ni 210H) supplied by INCO (Canada). Characterization of the as-received commercial powders was carried out using different techniques: particle size determination (d_{v50}) by Dynamic Light Scattering in a Mastersizer S (Malvern, Germany); specific surface, by adsorption/desorption N_2 gas in a Monosorb Surface Area (Quantachrome Co., USA); density was measured using a Monosorb Helium Multipycnometer (Quantachrome Co., USA). The average values of particles sizes (d_{BET}) were calculated from specific surface area measurements, assuming spherical, homogeneous primary particles, through the equation (1), where S_{BET} is the measured specific surface and ρ is the density of the powder [22]:

$$d_{BET} = \frac{6}{S_{BET} \cdot \rho} \quad (1)$$

Ti(C,N) (100 % Ti(C,N)) and FeNi (100 % FeNi) suspensions were prepared from those commercial powders in order to determine the rheological behavior of the suspensions using a Haake Mars (Thermo Scientific, Germany). The measurements were performed in control rate (CR) conditions using a double-cone plate with a diameter of 60 mm and angle of 2° (DC60/2°). After milling, both suspensions were mixed to fit the desired final composition of the cermet (hereafter called 15FeNi), which consist in an 85/15 vol.% of ceramic /metal phases. The metallic binder was designed with a fixed composition of 85/15 wt.% of Fe/Ni.

By simple volumetric mixing, 15FeNi stable aqueous suspension was prepared to obtain samples using a combination of colloidal and powder metallurgical techniques. Green bodies were processed by slip casting using a porous cast (SC). Additionally, in order to evaluate the effect of increasing the green density on the final mechanical properties of the sintered materials, some SC samples were subjected to an additional cold isostatic pressing step (SC-CIP). On the other hand, high solid content suspensions also were sprayed dried in order to obtain granules using a Labplant SD-05 (North Yorkshire, UK) with the main controlled operating parameters such as the temperature at the inlet (190 °C) and at the outlet (100 °C), the slurry pump rate (2 L/h), the air flow (29 m^3/h), and the atomizing nozzle design set to provide spherical agglomerates. These granules were pressed in a uniaxial die into cylinders of 16 mm of diameter, at 600 MPa (SDP process). All green compacts, listed in Table 1, were sintered in vacuum at 1450 °C for 120 minutes. All thermal treatments included a dwell of 30 minutes at 800 °C.

Table 1: Identification of samples prepared for each route

Route	Nomenclature
SC	*
SC-CIP	SC-CIP 15FeNi
SDP	SDP 15FeNi

*SC 15FeNi samples broke during sintering

The dimensions of the samples were used to measure the green density (ρ_{green}) and geometrical density after sintering (ρ_{geo}). Pycnometric density of sintered samples was measured using a Monosorb Helium Multipycnometer (Quantachrome Co., USA) (ρ_{He}). Theoretical density was calculated from the rule of mixtures. Close porosity (referred as P_{close}) was estimated as the deviation between the theoretical and pycnometric densities determined for each sintered sample. On the other hand, the open porosity (called P_{open}) was determined through the deviation between the geometrical and pycnometric densities. Microstructural and fractographic analysis of samples were carried out using a XL30 Scanning Electron Microscope (Philips, Netherlands) and a Jeol JCM-6000Plus Neoscope™ Scanning Electron Microscope (Jeol Ltd., Japan) respectively.

Fracture toughness, K_{IC}

The fracture toughness (K_{IC}) of SDP 15FeNi samples was determined using the Single Edge V-Notch Beam method (SEVNB) on standard specimens (7 specimens batch) of dimensions 3x4x27 mm^3. A razor blade automatic machine was utilized to create the notch, which was sharpened to a radius of less than 5μm in order to minimize the influence of notch radius on K_{IC} values [23]. The notched specimens were the fractured in four-point bending under displacement rate of 0.1 mm/min (environmental conditions of 22.5 °C and 25 % RH) on a standard testing machine (Zwick Z010, Zwick/Roell, Ulm, Germany) according to EN-843-1 [24].

Biaxial flexural strength, B3B

The biaxial flexural strength was measured using the ball on three balls (B3B) test [25–27], where a fully polished disc specimen is supported on three balls and loaded symmetrically by a fourth ball. In this loading situation, the three-point support guarantees well-defined three point contacts. At the midpoint of the disc surface opposite to the loading ball a biaxial tensile stress state exists, which is used for the biaxial strength testing. This test has been recognized to be very tolerant for some out of flatness of the disc and also for other small geometries or some misalignment. Furthermore, friction is recognized to be much smaller than in the commonly used bending tests. For these reasons, the B3B-test can also be used in as-sintered and small specimens. Details about the test can be found elsewhere [26].

In our case all four balls had a diameter of 9.524 mm and 6.35 mm depending of the diameter of the samples. The tensile loaded surfaces of the B3B specimens (disks of 1.2 mm in thickness and 13 mm in diameter for the SDP and 9 mm in diameter for the SC-CIP) were carefully grinded and polished to 1 microns finish to reach the same surface quality. The biaxial flexural test was carried out using an electro mechanic universal testing machine (Model 5505, Instron Ltd.) A pre-load of 10 N was applied to hold

the specimen between the four balls. The tests were conducted under load control at a rate of 100 N/s at room temperature (34 % RH at 23 °C). The load was increased until fracture and the fracture load, F, was used to calculate the maximum tensile biaxial stress in the specimen at the moment of fracture. To allow a proper statistical evaluation thirty specimens of each kind were tested. For an elastically isotropic material the maximum stress σ_{max} corresponding to the fracture load can be calculated as follows:

$$\sigma_{max} = f \cdot \frac{F}{t^2} \quad (2)$$

where *t* is the thickness of the disc and f a dimensionless factor, which depends on the geometry of the specimen and the balls, the Poisson's ratio of the tested material and details of the load transfer from the jig into the specimen [25]. The factor f was calculated for each geometry using a Mathematica applet (accessed in [28]). For the specimens of study (with thickness around 1.2 mm) the factor f ranged between 1.75 and 2. The maximal stress is located in the center of the three balls. It can be inferred from the referred figure that the central region, i.e. approx. 1/20 of the specimen dimension, is stressed with more than 90 % of the maximal stress. Therefore, localized strength measurements can be performed. We draw the attention of the reader that both the effective surface and volume in the B3B configuration are much smaller than under uniaxial bending.

Results and discussion

Characterization of the as received commercial powders

Table 2 summarizes the powder distribution size (dv_{50} and d_{BET}), specific area and density. Even though raw powders present similar d_{v50} values, their d_{BET} and specific surfaces differs quite remarkably: this is due to their different morphologies and particle size distribution. While the Fe powder presents a spherical morphology and a narrow distribution, Ti(C,N) and Ni powders show an irregular shape as well as a wide particle size distribution.

Table 2: Powder distribution size (dv_{50} and d_{BET}), specific area and density of the as-received powders.

Powder	Distribution Size		Specific surface area*	Density**
	dv_{50}	d_{BET}		
Ti(C,N)	2.1 µm	0.4 µm	3.0 m^2/g	5.1 g/cm^3
Fe	3.5 µm	1.2 µm	0.6 m^2/g	7.8 g/cm^3
Ni	1.7 µm	0.2 µm	4.0 m^2/g	8.9 g/cm^3

* ± 0.1 Standard deviation in density measurements

** ± 0.1 Standard deviation in specific area measurements

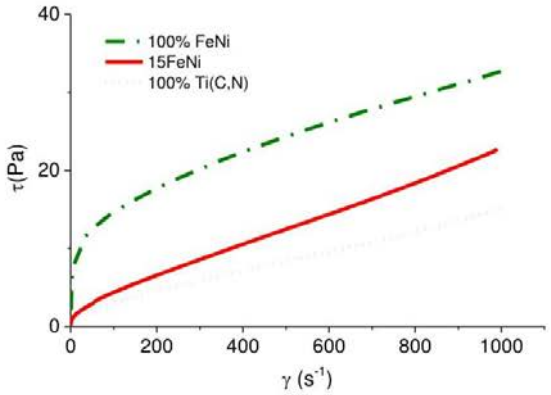

Figure 1: Flow curves of 100 % Ti(C,N), 100 % FeNi and 15FeNi

Processing of cermet samples

High solid content suspensions were prepared according to the conditions described elsewhere [29]. Fig. 1 shows the results of the rheological study under optimized conditions of the final suspension Ti(C,N)-FeNi, compared to the slurries of the starting constituents. As it can be observed, in all cases, viscosity decreases under shear strain, presenting a shear thinning (pseudoplastic) behavior. At highest levels of shear rate, suspensions seem to show a Newtonian behavior.

The 15FeNi suspension was used to prepare bulk pieces as described in Experimental Part. After sintering, SC-CIP and SDP samples were mounted and polished in order to carry out the pertinent microstructural analysis. However, the low structural integrity of SC samples, due to their high amount of porosity, caused the samples not to withstand the sintering cycle and break. Fig. 2 shows the broken sintered SC samples as well as the microstructure of sintered materials (SC-CIP and SDP). All micrographs allows identifying two different phases in the cermet: the brighter phase corresponds to the FeNi matrix and the darker phase represents the ceramic Ti(C,N) phase. The two phases are homogeneously distributed and interconnected; however, depending of the processing method, each sample shows remnant porosity, as it can also be corroborated in Table 3. Attending to the results exposed in both Table 3 and Fig. 2, SC-CIP samples show a higher porosity degree and a worse phase distribution than samples obtained through SDP.

Table 3: Density, porosity and biaxial strength of the investigated samples.

Material	ρ^{*}_{green} (g/cm^3)	ρ^{**}_{He} (g/cm^3)	ρ^{**}_{geo} (g/cm^3)	ρ_{th} (g/cm^3)	P_{tot} (%)	P_{close} (%)	P_{open} (%)	Characteristic strength (MPa)
SC 15FeNi	3.03	---	---		---	---	---	---
SC-CIP 15FeNi	3.69	5.40	5.38	5.53	2.75	2.44	0.31	1374
SDP 15FeNi	3.81	5.47	5.46		1.15	1.14	0.01	1529

*** ± 0.1 Standard deviation in green density measurements**

**** ± 0.1 Standard deviation in sintered density measurements**

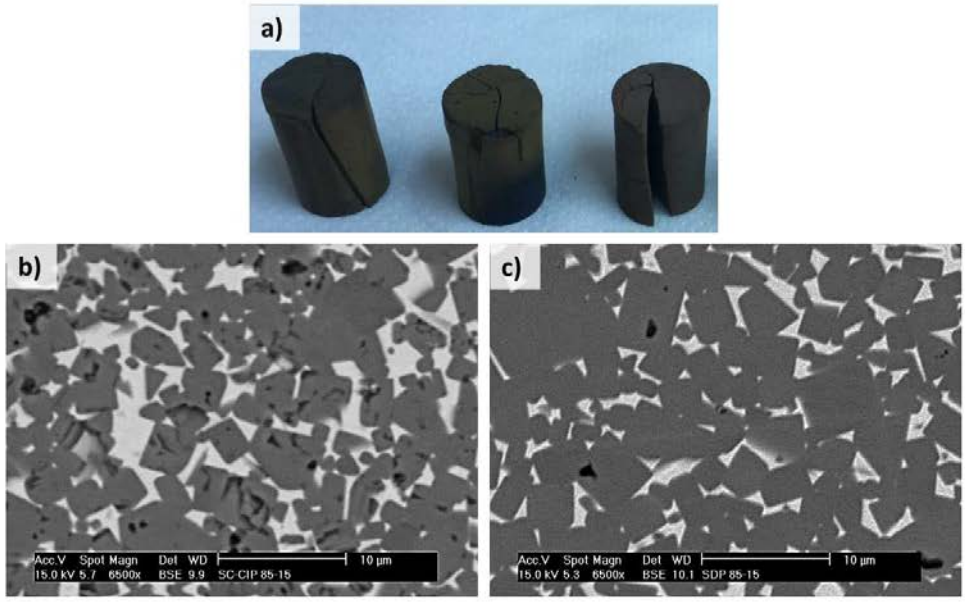

Figure 2: (a) Sintered SC cylinders broken during sintering, (b) SEM micrographs of SC-CIP 15FeNi and (c) SDP 15FeNi microstructures.

Mechanical characterization of samples

The fracture toughness was only evaluated on SDP 15FeNi samples following the VAMAS procedure on pre-notched specimens [30] as it can be seen in the Fig. 3. This material presents a mean value of 12.2 ± 0.3 MPa·m$^{1/2}$. A general overview of the fracture surface (macroscopic and microscopic) is shown in the Fig. 3a and Fig. 3b (red inset) respectively. Going to higher magnifications in Fig. 3c (blue inset), is shown a high resolution micrograph of the fracture surface of the composite. Cermet exhibits brittle fracture behavior on the macro-level, but on the micro-level both the brittle fracture of the ceramic phase and the ductile fracture of the binder phase are observed. This brittle fracture of the ceramic phase follows a transgranular mode of fracture, as characterized by the typical river-like pattern. On the other hand, the fracture along to the carbide-binder interface has remnants of the plastically fractured binder phase with shallow dimples on the smooth surface of the carbide.

The mechanical strength of cermets is very sensitive to the size and location of critical flaws, as it is the case of brittle materials. Typical volume flaws, which may act as fracture origins, are pores, impurity inclusions, lakes of binder, agglomerates, etc. In order to identify the type of critical defect, a fractographic analysis was performed in selected samples as it is shown in Fig. 4. In most of the samples investigated in this work, the fracture origin resulted to be a large pore in the surface and/or subsurface of our materials, which on a mesoscale, may be modelled by a spherical cavity with a radius of about 30 µm.

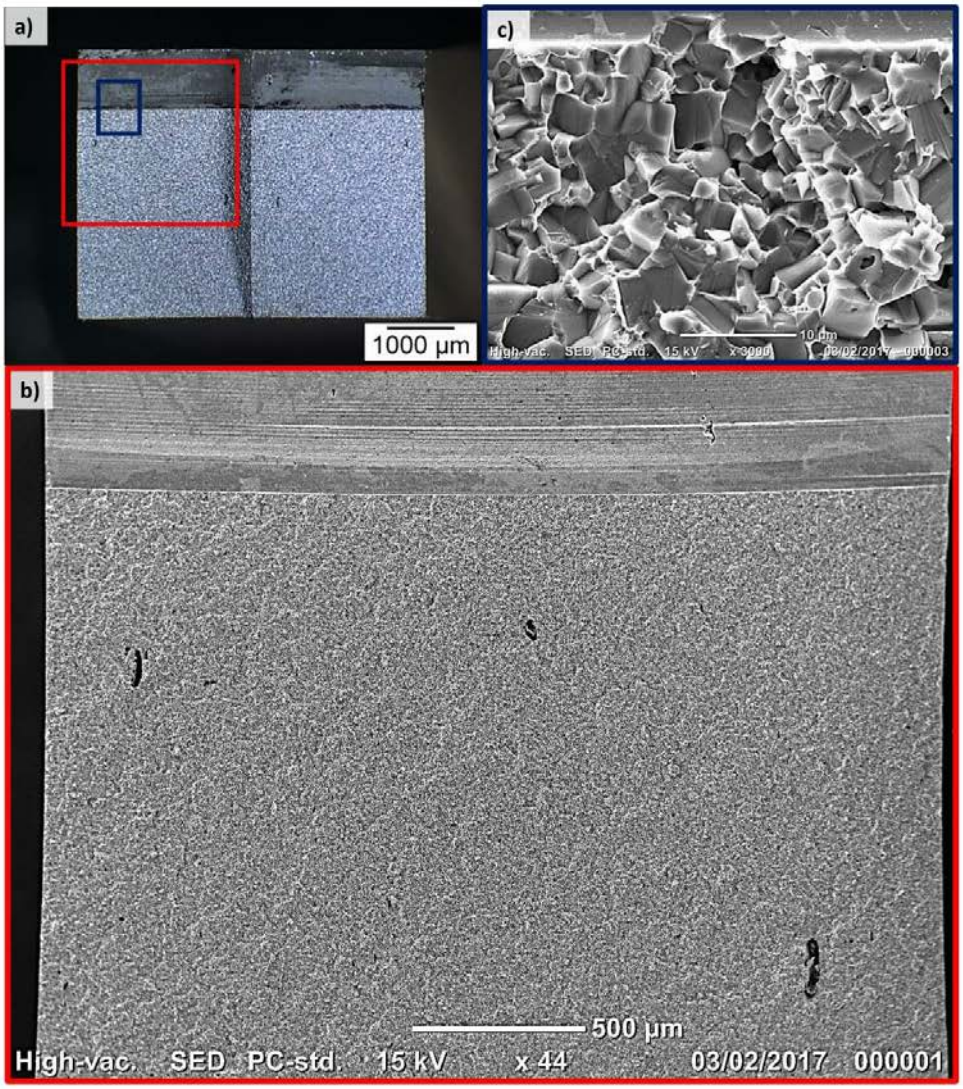

Figure 3: Fracture surface of a notched SDP 15FeNi cermet specimen fractured in 4-point bending (a) Macroscopic view (b) SEM micrograph of fracture morphology of sintered SDP 15FeNi cermet and (c) Zoom of fracture surface

Macroscopic brittle fracture was controlled by the extension of small flaws that were dispersed in the material and which behave like cracks. As it was explained in the previous section, there is a strong correlation between the processing route and the appearance of critical flaws (see Table 3). As a consequence, the biaxial strength of the Ti(C,N)-FeNi composites fabricated through the SDP process showed a relatively high characteristic strength value of 1529 MPa, as compared to the characteristic strength of the SC-CIP, 1374 MPa.

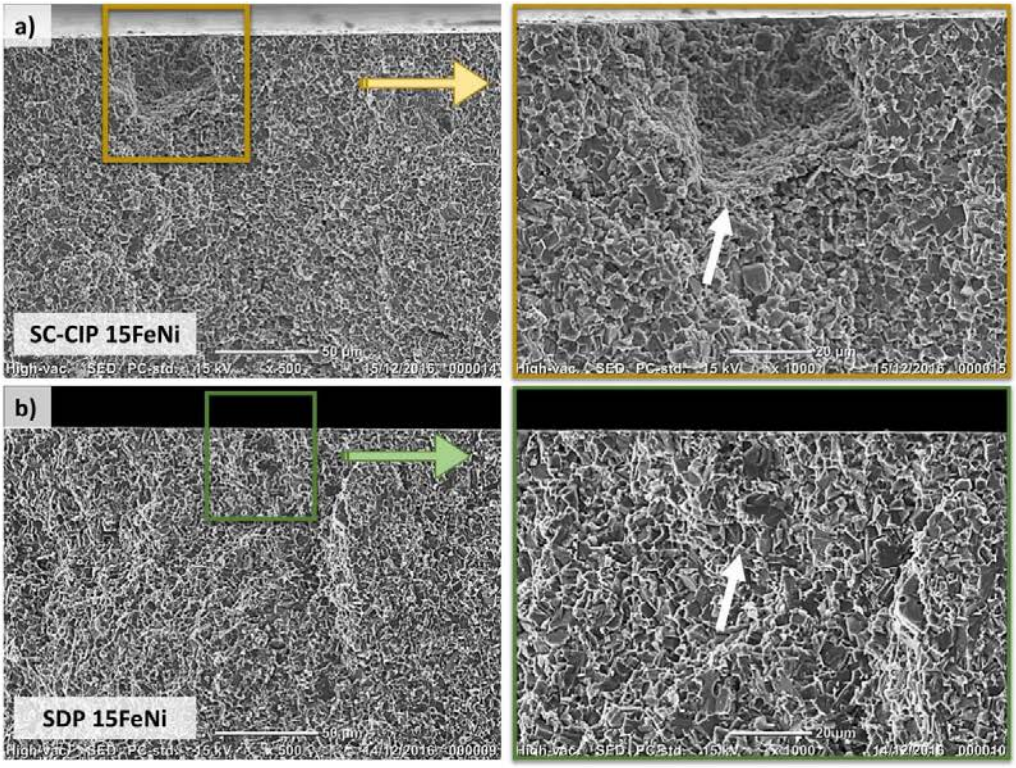

Figure 4: Fracture origins of (a) SC-CIP 15FeNi and (b) SDP 15FeNi specimens. The tensile surface is at the top of the micrographs.

Summary and conclusions

In this research work, the effect of combining colloidal and powder metallurgy techniques on the microstructure and mechanical properties of sintered Ti(C,N)-based cermets was investigated. The following conclusions can be drawn:

- Through rheological studies, stable aqueous high solid content suspensions of Ti(C,N) (45 vol.%) and FeNi (35 vol.%) were prepared. Then, those suspensions were mixed in order to obtain the desired final composition of the cermet (85/15 vol.% Ti(C,N)-FeNi). The rheological behavior of this final suspension fits the conditions to be processed by Slip Casting as well as by SDP (region from 150 to 100 s^{-1}).
- The combination of colloidal and powder metallurgy techniques allow us to explore a wide range of possibilities for the processing of bulk samples from those stable suspensions.
- The fracture process is largely influenced by the local microstructure and the presence of flaws created during the processing of samples.
- Considerably improved biaxial strength resistance was observed for SDP cermets (1529 MPa) when compared to the alternative routes developed in this research work (for example SC-CIP, 1374 MPa). This result is mainly caused by the reduction of the size of defects in this microstructure.

Acknowledgements

The authors acknowledge the financial support from the Spanish Government through the projectsMAT2015-70780-C4-1-P and MAT2015-70780-C4-2-P, the Regional Government of Madrid through the program MULTIMAT-CHALLENGE, ref. S2013/MIT-2862. M. Dios acknowledges MINECO through the grant BES-2013-065760.

References

1. A. Bellosi, R. Calzavarini, M.G. Faga, F. Monteverde, C. Zancolò, G.E. D'Errico, Characterisation and application of titanium carbonitride-based cutting tools, in: J. Mater. Process. Technol., 2003. doi:10.1016/S0924-0136(03)00339-X
2. P. Ettmayer, H. Kolaska, W. Lengauer, K. Dreyer, Ti(C,N) cermets — Metallurgy and properties, Int. J. Refract. Met. Hard Mater. 13 (1995) 343–351. doi:10.1016/0263-4368(95)00027-G
3. Y. Peng, H. Miao, Z. Peng, Development of TiCN-based cermets: Mechanical properties and wear mechanism, RMHM. 39 (2013) 78–89. doi:10.1016/j.ijrmhm.2012.07.001
4. K. Aigner, W. Lengauer, P. Ettmayer, Interactions in iron-based cermet systems, J. Alloys Compd. 262–263 (1997) 486–491. doi:10.1016/S0925-8388(97)00360-5
5. M. Chen, Q. Zhuang, N. Lin, Y. He, Improvement in microstructure and mechanical properties of Ti(C,N)-Fe cermets with the carbon additions, J. Alloys Compd. 701 (2017) 408–415, doi:10.1016/j.jallcom.2017.01.119
6. H. Yu, Y. Liu, Y. Jin, J. Ye, Effect of secondary carbides addition on the microstructure and mechanical properties of (Ti, W, Mo, V)(C, N)-based cermets, Int. J. Refract. Met. Hard Mater. 29 (2011) 586–590. doi:10.1016/j.ijrmhm.2011.03.013
7. E. Chicardi, Y. Torres, M.J. Sayagués, V. Medri, C. Melandri, J.M. Córdoba, F.J. Gotor, Toughening of complete solid solution cermets by graphite addition, Chem. Eng. J. 267 (2015) 297–305. doi:10.1016/j.cej.2015.01.022
8. P. Alvaredo, J.J. Roa, E. Jiménez-Pique, L. Llanes, E. Gordo, Characterization of interfaces between TiCN and iron-base binders, Int. J. Refract. Met. Hard Mater. 63 (2017) 32–37. doi:10.1016/j.ijrmhm.2016.08.010
9. P. Alvaredo, M. Dios, B. Ferrari, E. Gordo, Interface study for the design of alternative matrixes in cermets, in: Eur. Congr. Exhib., Reims, n.d
10. R. Licheri, R. Orrù, G. Cao, A. Crippa, R. Scholz, Self-propagating combustion synthesis and plasma spraying deposition of TiC–Fe powders, Ceram. Int. 29 (2003) 519–526. doi:10.1016/S0272-8842(02)00196-7
11. E.A. Levashov, A.S. Mukasyan, A.S. Rogachev, D. V Shtansky, Self-propagating high-temperature synthesis of advanced materials and coatings, Int. Mater. Rev. 62 (2017) 203–239. doi:10.1080/09506608.2016.1243291
12. E. Chicardi, F.J. Gotor, V. Medri, S. Guicciardi, S. Lascano, J.M. Córdoba, Hot-pressing of (Ti, Mt)(C, N)–Co–Mo 2 C (Mt = Ta, Nb) powdered cermets synthesized by a mechanically induced self-sustaining reaction, Chem. Eng. J. 292 (2016) 51–61. doi:10.1016/j.cej.2016.02.007

13. I.W. Brown, W. Owers, Fabrication, microstructure and properties of Fe–TiC ceramic–metal composites, Curr. Appl. Phys. 4 (2004) 171–174. doi:10.1016/j.cap.2003.11.001

14. S. Park, S. Kang, Toughened ultra-fine (Ti,W)(CN)–Ni cermets, Scr. Mater. 52 (2005) 129–133. doi:10.1016/j.scriptamat.2004.09.017

15. A. Jam, L. Nikzad, M. Razavi, TiC-based cermet prepared by high-energy ball-milling and reactive spark plasma sintering, Ceram. Int. 43 (2017) 2448–2455. doi:10.1016/j.ceramint.2016.11.039

16. J. Xiong, Z. Guo, M. Yang, B. Shen, Preparation of ultra-fine TiC0.7N0.3-based cermet, Int. J. Refract. Met. Hard Mater. 26 (2008) 212–219. doi:10.1016/j.ijrmhm.2007.05.001

17. S. Cabanas-Polo, R. Bermejo, B. Ferrari, A.J. Sanchez-Herencia, Ni–NiO composites obtained by controlled oxidation of green compacts, Corros. Sci. 55 (2012) 172–179. doi:10.1016/j.corsci.2011.10.016

18. J.A. Escribano, J.L. García, P. Alvaredo, B. Ferrari, E. Gordo, A.J. Sanchez-Herencia, FGM stainless steel-Ti(C,N) cermets through colloidal processing, Int. J. Refract. Met. Hard Mater. 49 (2015) 143–152. doi:10.1016/j.ijrmhm.2014.05.008

19. N. Hernández, A.J. Sánchez-Herencia, R. Moreno, Forming of nickel compacts by a colloidal filtration route, Acta Mater. 53 (2005) 919–925. doi:10.1016/j.actamat.2004.10.038

20. N. Hernández, R. Moreno, A.J. Sánchez-Herencia, J.L.G. Fierro, Surface behavior of nickel powders in aqueous suspensions, J Phys Chem B. 109 (2005) 4470–4474. doi:10.1021/jp0448954

21. Z. Guo, J. Xiong, M. Yang, S. Xiong, J. Chen, Y. Wu, H. Fan, L. Sun, J. Wang, H. Wang, Dispersion of nano-TiN powder in aqueous media, J. Alloys Compd. 493 (2010) 362–367. doi:10.1016/j.jallcom.2009.12.103

22. B. Kear, J. Colaizzi, W. Mayo, S.-C. Liao, On the processing of nanocrystalline and nanocomposite ceramics, Scr. Mater. 44 (2001) 2065–2068. doi:10.1016/S1359-6462(01)00884-3

23. R. Damani, R. Gstrein, R. Danzer, Critical notch-root radius effect in SENB-S fracture toughness testing, J. Eur. Ceram. Soc. 16 (1996) 695–702. doi:10.1016/0955-2219(95)00197-2

24. ENV 843-1 Advanced technical ceramics – monolithic ceramics – mechanical tests at room temperature – Part 1: determination of flexural strength. 1995, (n.d.)

25. A. Börger, P. Supancic, R. Danzer, The ball on three balls test for strength testing of brittle discs: stress distribution in the disc, J. Eur. Ceram. Soc. 22 (2002) 1425–1436. doi:10.1016/S0955-2219(01)00458-7

26. A. Börger, P. Supancic, R. Danzer, The ball on three balls test for strength testing of brittle discs: Part II: analysis of possible errors in the strength determination, J. Eur. Ceram. Soc. 24 (2004) 2917–2928. doi:10.1016/j.jeurceramsoc.2003.10.035

27. R. Danzer, W. Harrer, P. Supancic, T. Lube, Z. Wang, A. Börger, The ball on three balls test—Strength and failure analysis of different materials, J. Eur. Ceram. Soc. 27 (2007) 1481–1485. doi:10.1016/j.jeurceramsoc.2006.05.034

28. BALL-ON-3-BALLS TEST (B3B) – STRENGTH TESTING APP, (n.d.). http://www.isfk.at/de/960/

29. M. Dios, Z. Gonzalez, P. Alvaredo, E. Gordo, R. Bermejo, B. Ferrari, Novel colloidal approach for the microstructural improvement in Ti(C,N)/FeNi cermets, Acta Mater. (2017)

30. ISO/DIS 23146 Fine ceramics (advanced ceramics, advanced technical ceramics) – test methods for fracture toughness of monolithic ceramics – single-edge V-notch beam (SEVNB) method. 2007, (n.d.)